



# Impact of NO<sub>x</sub> and OH on secondary organic aerosol formation from β-pinene photooxidation

Mehrnaz Sarrafzadeh<sup>1,3</sup>, Jürgen Wildt<sup>2,1</sup>, Iida Pullinen<sup>1</sup>, Monika Springer<sup>1</sup>, Einhard Kleist<sup>2</sup>, Ralf Tillmann<sup>1</sup>, Sebastian H. Schmitt<sup>1</sup>, Cheng Wu<sup>1</sup>, Thomas F. Mentel<sup>1</sup>, Defeng Zhao<sup>1</sup>, Donald R. Hastie<sup>3</sup>, and Astrid Kiendler-Scharr<sup>1</sup>

<sup>1</sup>Institute for Energy and Climate Research, IEK-8, Forschungszentrum Jülich, 52425 Jülich, Germany

<sup>2</sup>Institute of Bio- and Geosciences, IBG-2, Forschungszentrum Jülich, 52425 Jülich, Germany

<sup>3</sup>Centre for Atmospheric Chemistry, York University, 4700 Keele St., Toronto, ON M3J 1P3, Canada

Correspondence to: Jürgen Wildt (j.wildt@fz-juelich.de)

Received: 18 April 2016 – Published in Atmos. Chem. Phys. Discuss.: 27 April 2016

Revised: 19 July 2016 – Accepted: 18 August 2016 – Published: 12 September 2016

**Abstract.** In this study, the NO<sub>x</sub> dependence of secondary organic aerosol (SOA) formation from photooxidation of the biogenic volatile organic compound (BVOC) β-pinene was comprehensively investigated in the Jülich Plant Atmosphere Chamber. Consistent with the results of previous NO<sub>x</sub> studies we found increases of SOA yields with increasing [NO<sub>x</sub>] at low-NO<sub>x</sub> conditions ([NO<sub>x</sub>]<sub>0</sub> < 30 ppb, [BVOC]<sub>0</sub> / [NO<sub>x</sub>]<sub>0</sub> > 10 ppbC ppb<sup>-1</sup>). Furthermore, increasing [NO<sub>x</sub>] at high-NO<sub>x</sub> conditions ([NO<sub>x</sub>]<sub>0</sub> > 30 ppb, [BVOC]<sub>0</sub> / [NO<sub>x</sub>]<sub>0</sub> ~ 10 to ~ 2.6 ppbC ppb<sup>-1</sup>) suppressed the SOA yield. The increase of SOA yield at low-NO<sub>x</sub> conditions was attributed to an increase of OH concentration, most probably by OH recycling in NO + HO<sub>2</sub> → NO<sub>2</sub> + OH reaction. Separate measurements without NO<sub>x</sub> addition but with different OH primary production rates confirmed the OH dependence of SOA yields. After removing the effect of OH concentration on SOA mass growth by keeping the OH concentration constant, SOA yields only decreased with increasing [NO<sub>x</sub>]. Measuring the NO<sub>x</sub> dependence of SOA yields at lower [NO] / [NO<sub>2</sub>] ratio showed less pronounced increase in both OH concentration and SOA yield. This result was consistent with our assumption of OH recycling by NO and to SOA yields being dependent on OH concentrations. Our results furthermore indicated that NO<sub>x</sub> dependencies vary for different NO<sub>x</sub> compositions. A substantial fraction of the NO<sub>x</sub>-induced decrease of SOA yields at high-NO<sub>x</sub> conditions was caused by NO<sub>x</sub>-induced suppression of new particle formation (NPF), which subsequently limits the particle surface where low volatiles condense. This was

shown by probing the NO<sub>x</sub> dependence of SOA formation in the presence of seed particles. After eliminating the effect of NO<sub>x</sub>-induced suppression of NPF and NO<sub>x</sub>-induced changes of OH concentrations, the remaining effect of NO<sub>x</sub> on the SOA yield from β-pinene photooxidation was moderate. Compared to β-pinene, the SOA formation from α-pinene photooxidation was only suppressed by increasing NO<sub>x</sub>. However, basic mechanisms of the NO<sub>x</sub> impacts were the same as that of β-pinene.

## 1 Introduction

Biogenic volatile organic compounds (BVOCs), such as monoterpenes (C<sub>10</sub>H<sub>16</sub>) are emitted in large quantities into the atmosphere (Guenther et al., 1995, 2012; Griffin et al., 1999a). These BVOCs are oxidized in the atmosphere by hydroxyl radicals (OH), ozone (O<sub>3</sub>) or nitrate radicals (NO<sub>3</sub>) resulting in the formation of secondary organic aerosol (SOA). SOA contributes to a substantial fraction of ambient organic aerosol and is known to adversely affect visibility, climate and human health (Hallquist et al., 2009).

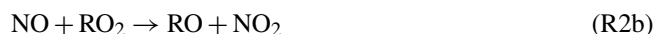
SOA formation potentials of BVOC species are represented by SOA yields, which are generally defined as the ratio of the SOA mass produced from the oxidation of the SOA precursor to the mass of the precursor consumed (Odum et al., 1996). Despite the fact that many studies have focused on the production of SOA from a number of monoterpenes, reported SOA yields have shown high variability for a given

precursor (Pandis et al., 1991; Hoffmann et al., 1997; Griffin et al., 1999b; Larsen et al., 2001; Presto et al., 2005; Kroll et al., 2006; Ng et al., 2007a; Mentel et al., 2009; Eddingsaas et al., 2012a). For instance, the reported SOA mass yield for  $\alpha$ -pinene photooxidation ranges from 8 to 37 % (Eddingsaas et al., 2012a). This variability is likely related to the numerous factors that influence the SOA yields, such as the inorganic and organic mass loading, particle acidity, NO<sub>x</sub> (NO<sub>x</sub> = NO + NO<sub>2</sub>) level, humidity, and temperature. Therefore, ambient SOA yields cannot be represented by a unique value for a given monoterpene as the yields are heavily dependent on the conditions under which the SOA is formed.

One of the critical factors is the impact of NO<sub>x</sub> on SOA formation. For sesquiterpenes, such as longifolene and aromadendrene, yields increase with increasing NO<sub>x</sub> (Ng et al., 2007a). However, results of the majority of studies indicate that SOA yields are lower at high-NO<sub>x</sub> levels (Hatakeyama et al., 1991; Pandis et al., 1991; Presto et al., 2005; Kroll et al., 2006; Ng et al., 2007a). It is generally assumed that the impact of NO<sub>x</sub> results from altering the balance between competing peroxy-radical (RO<sub>2</sub>) reactions and thus from the changes in the distribution of oxidation products. Reaction (R1) is the dominant pathway for RO<sub>2</sub> radicals under low-NO<sub>x</sub> conditions, which leads to the formation of low-volatility hydroperoxides that can participate in new particle formation (NPF) and contribute to SOA mass (Johnson et al., 2005; Camredon et al., 2007).



Under high-NO<sub>x</sub> conditions, RO<sub>2</sub> radicals react with NO resulting in the formation of organic nitrates (Reaction R2a) as well as alkoxy radicals (Reaction R2b) that either fragment, or react to form more volatile products. This understanding implies that higher NO<sub>x</sub> concentrations will suppress the formation of low volatility products, and thereby suppress NPF and SOA mass formation.



Despite numerous studies of SOA formation from terpene ozonolysis, the SOA formation from OH oxidation of  $\beta$ -pinene has been scarcely investigated. In the present study, we investigated the SOA formation from  $\beta$ -pinene photooxidation under varied NO<sub>x</sub> levels in the Jülich Plant Atmosphere Chamber (JPAC) to gain more insight into the impact of NO<sub>x</sub> on SOA yield and to better characterize mechanisms leading to effects of NO<sub>x</sub> on SOA yield.

## 2 Experimental

The experimental setup of JPAC is described in detail elsewhere (Mentel et al., 2009, 2015). The chamber is 1450 L in

volume, made of borosilicate glass and set up in a climate-controlled housing. Temperature and relative humidity inside the chamber were held constant at  $16 \pm 1$  °C and  $63 \pm 2$  % respectively over the course of the experiments. The chamber was operated as a continuously stirred tank reactor with a residence time of approximately 46 min. The flow into the chamber consisted of two purified air streams. One stream was passed through an ozonator and was humidified with double distilled water. The other stream contained  $\beta$ -pinene emitted from a diffusion/permeation source held at 38 °C. Where necessary seed particles could be generated externally and introduced using a third air stream.

The chamber was equipped with several lamps: 12 discharge lamps (HQI 400 W/D; Osram) used to simulate the solar light spectrum. Twelve discharge lamps (Philips, TL 60 W/10-R, 60 W,  $\lambda_{\text{max}} = 365$  nm) were used for NO<sub>2</sub> photolysis. According to the spectral distribution of their light these lamps are termed as UVA lamps from here on. The TUV lamp could be shielded by glass tubes to control the amount of UV radiation entering the chamber. Thus, by altering the gap between these glass tubes, the OH production rate could be adjusted by varying the photolysis rate  $J(\text{O}^1\text{D})$ . It has to be noted that the short wavelength cut off of the glass is around 350 nm and thus no light with wavelength short enough to produce O<sup>1</sup>D is in the chamber when the TUV lamp is off. Furthermore, the absorption cross section of NO<sub>2</sub> at the wavelength of the TUV lamp is more than an order of magnitude lower than at wavelengths around 365 nm (Davidson et al., 1988). Together with the quite low energy of the TUV lamp compared to the energy of the UVA lamps, this allowed varying  $J(\text{O}^1\text{D})$  and  $J(\text{NO}_2)$  independent of each other.

A suite of instruments were used to measure both the gas and particle phase products. Ozone concentration was determined by UV photometric devices (Thermo Environmental 49 and Ansyco, O<sub>3</sub> 42M ozone analyzers), NO was measured by chemiluminescence (Eco Physics, CLD 770 AL ppt), NO<sub>2</sub> by chemiluminescence after photolysis (Eco Physics, PLC 760) and relative humidity was measured by a dew point mirror (TS-2, Walz). Furthermore, a condensation particle counter (CPC; TSI 3783) and a scanning mobility particle sizer (SMPS; combination of a TSI 3081 electrostatic classifier and a TSI 3025 CPC) were used to count the total particle number greater than 3 nm and to measure the particle size distribution between 13 and 740 nm respectively. The total particle mass concentration was estimated from the measured total aerosol volume assuming a SOA density of  $\sim 1.2$  g cm<sup>-3</sup> and spherical particles.  $\beta$ -pinene mixing ratio in the chamber was determined by gas chromatography–mass spectrometry (GC-MS; Agilent GC-MSD system with HP6890 GC and 5973 MSD) and a proton transfer reaction mass spectrometer (PTR-MS; Ionicon). The GC-MS and PTR-MS were switched periodically between the outlet and the inlet of the chamber to quantify concentrations of  $\beta$ -pinene entering and exiting the chamber. The OH concentra-

tion was estimated from the decay of  $\beta$ -pinene in the chamber (Eq. 2) (Kiendler-Scharr et al., 2009).

$$\frac{d[\beta p]}{dt} = \frac{F}{V} \cdot ([\beta p]_{\text{in}} - [\beta p]) - \left( k^{\text{OH}} \cdot [\text{OH}] + k^{\text{O}_3} \cdot [\text{O}_3] \right) \cdot [\beta p] \quad (1)$$

$$[\text{OH}] = \frac{\frac{F}{V} \cdot \frac{[\beta p]_{\text{in}} - [\beta p]}{[\beta p]} - k^{\text{O}_3} \cdot [\text{O}_3]}{k^{\text{OH}}} \quad (2)$$

Equation (1) is the basic rate equation for a continuously stirred tank reactor resulting from mass balance and Eq. (2) results from Eq. (1) under steady state conditions when solving for [OH]. In Eqs. (1) and (2),  $V$  is the volume of the chamber and  $F$  is the total air flow through the chamber.  $[\beta p]_{\text{in}}$  and  $[\beta p]$  are the concentrations of  $\beta$ -pinene in the inlet air and in the chamber respectively. For a well-mixed continuously stirred tank reactor,  $[\beta p]$  is the concentration of  $\beta$ -pinene measured in the outlet flow.  $k^{\text{OH}}$  and  $k^{\text{O}_3}$  are the rate constants of reactions of  $\beta$ -pinene with OH and with O<sub>3</sub>. Since  $\beta$ -pinene has a quite low rate constant with O<sub>3</sub> ( $k^{\text{O}_3} = 1.5 \times 10^{-17} \text{ cm}^3 \text{ s}^{-1}$ ; Atkinson and Arey, 2003), the reaction of  $\beta$ -pinene with O<sub>3</sub> could be neglected from Eq. (2) for our ozone- (50–100 ppb) and OH concentrations ( $9 \times 10^6$ – $1.6 \times 10^8 \text{ cm}^{-3}$ ). The uncertainty in OH concentration was estimated to be approximately 20 % (Wildt et al., 2014).

SOA yields were determined as described in Mentel et al. (2009). Particle formation was induced by switching on ozone photolysis and thus producing OH radicals. From such a measurement the formed particle mass as well as the amount of consumed BVOC was obtained. Repeating such experiments using different amounts of BVOC gave a set of data on SOA mass and consumed BVOC. Plotting the SOA masses in dependence of consumed BVOC gave linear relationships with only small deviations from linearity. The slopes of such plots were used as the incremental yields. However, different from the procedure described in Mentel et al. (2009), here we use particle masses corrected for wall losses of extremely low volatile organic compounds (ELVOCs) that are direct particle precursors.

Details of the correction method are described in detail in the supplement. Briefly, ELVOCs were measured with a NO<sub>3</sub><sup>-</sup>-CIMS (Ehn et al., 2014; Mentel et al., 2015). Stopping the ELVOC production by stopping OH production allowed for the measurement of their decay rates and thus their lifetimes. In the absence of particles, the lifetimes were in the range of 2 to 3 min. The lifetimes became shorter with increasing particle surface because of condensation of the ELVOCs onto the particles. Knowing the total loss rate and the wall loss rate allowed for the determination of ELVOC condensation onto the particles, as well as the fraction of condensation  $F_p$ :  $\left( F_p = \frac{\text{Loss on particles}}{\text{Loss on particles} + \text{loss on walls}} \right)$ . The measured mass was then corrected accordingly, by dividing by  $F_p$ . We verified this correction procedure for experiments with  $\alpha$ -pinene and  $\beta$ -pinene with particle surfaces varying

over a wide range, including different amounts of ammonium sulfate seed aerosols. Note that the numbers obtained for wall loss correction are only valid for the chamber used in this study.

Additionally, we used another approach to determine the mass yields at steady state conditions. Correcting measured particle masses by the procedure described in the supplement, revealed that after an induction time of  $\sim 20$  min, the wall loss corrected particle mass was constant as long as the OH production rate was constant. This allowed determining yields using steady state assumptions. Yields were determined by dividing the particle mass formed in the experiment by the oxidation rate of the BVOC. With our method of [OH] determination, using the BVOC consumption according to Eq. (2), and at the negligible inflow of particle mass into the chamber, this equals the simple mass balance assumption: produced particle mass divided by BVOC consumption (Eq. 3).

$$Y = \frac{\text{Particle mass}}{\text{BVOC consumption}} \quad (3)$$

As was expected from the consistency of wall loss corrected particle masses, both procedures of yield determinations led to identical results. However, the method using steady state conditions had advantages since adjustments of [OH] were required during many experiments. The justification to use both type of yield determinations is given in the supplement.

## Experimental procedure

A series of  $\beta$ -pinene photooxidation experiments were performed in the JPAC to investigate the SOA formation under low-NO<sub>x</sub> (here defined as  $[\text{NO}_x]_0 < 30$  ppb,  $[\text{BVOC}]_0 / [\text{NO}_x]_0 > 10$ ) and high-NO<sub>x</sub> (here defined as  $[\text{NO}_x]_0 > 30$  ppb,  $[\text{BVOC}]_0 / [\text{NO}_x]_0 < 10$ ) conditions. In these experiments, the inflow of  $\beta$ -pinene (95 %, Aldrich) to the chamber was kept constant, leading to initial mixing ratios of  $37 \pm 0.6$  ppb. Initial O<sub>3</sub> concentration was  $40 \pm 5$  ppb. NO<sub>2</sub> (Linde,  $104 \pm 3$  ppm NO<sub>2</sub> in nitrogen) was introduced into the  $\beta$ -pinene air stream. Initial NO<sub>x</sub> concentrations,  $[\text{NO}_x]_0$ , in the chamber were varied between  $< 1$  and 146 ppb. The chamber was illuminated with one of the HQI lamps and all the UVA lamps, resulting in an NO<sub>2</sub> photolysis frequency ( $J(\text{NO}_2)$ ) of  $4.3 \times 10^{-3} \text{ s}^{-1}$ . When VOC, NO<sub>x</sub> and O<sub>3</sub> concentrations in the chamber were near to steady state, the experiment was initiated by turning on the TUV lamp resulting in OH radical production. During the described experiments, a constant  $J(\text{O}^1\text{D})$  was maintained. Experiments without NO<sub>x</sub> addition were performed between NO<sub>x</sub> experiments. In these cases, residual NO<sub>x</sub> concentrations from chamber walls were below 1 ppb.

After initiating the OH production,  $\beta$ -pinene and NO<sub>x</sub> concentrations decreased due to their reactions with OH rad-

icals. The majority of the results presented in this study are from steady state measurements, when all physical and chemical parameters were constant in the chamber. However, for the purpose of comparison with the literature data, the initial concentration of NO<sub>x</sub>, [NO<sub>x</sub>]<sub>0</sub>, and β-pinene, [BVOC]<sub>0</sub>, were also used here.

To investigate the role of NO<sub>x</sub> on SOA formation in the presence of inorganic aerosol, β-pinene photooxidation / NO<sub>x</sub> experiments were repeated in the presence of seed aerosol. The seed particles were generated using a constant output aerosol generator (TSI, Model 3076) by atomizing (NH<sub>4</sub>)<sub>2</sub>SO<sub>4</sub> solutions (typical concentration ~ 40 mg L<sup>-1</sup>) at a pressure of around 1.4 bar. The generated aerosol then passed through a silica gel diffusion drier before entering the reaction chamber. In the control experiments, distilled water was used for atomization to keep the experimental conditions constant. For these experiments, the organic particle mass was determined by subtracting the initial seed aerosol mass from the total particle mass.

### 3 Results and discussion

#### 3.1 Impact of NO<sub>x</sub> on SOA formation

To determine the influence of NO<sub>x</sub> on SOA formation, a series of NO<sub>x</sub> experiments were conducted in the JPAC in which β-pinene was oxidized in the absence of inorganic seed aerosol. A summary of experimental conditions and results for the β-pinene / NO<sub>x</sub> photooxidation experiments is given in Table 1. Figure 1 shows SOA yields, calculated from wall-loss corrected maximum particle mass concentration (PM<sub>max</sub>), as a function of [BVOC]<sub>0</sub> / [NO<sub>x</sub>]<sub>0</sub> ratio and [NO<sub>x</sub>]<sub>0</sub>. The strong dependence of SOA yield on BVOC / NO<sub>x</sub> levels is evident. At low NO<sub>x</sub> conditions an increase in the initial NO<sub>x</sub> concentration increases the SOA yield, whereas at high-NO<sub>x</sub> concentrations the opposite SOA yield dependence on NO<sub>x</sub> was observed. Similar NO<sub>x</sub> dependencies of SOA yields have been observed in previous studies (Pandis et al., 1991; Kroll et al., 2006; Zhang et al., 1992; Camredon et al., 2007; Xu et al., 2014).

At high-NO<sub>x</sub> conditions strong depletion of SOA yield as well as NPF was observed with increasing NO<sub>x</sub> (Fig. 1). Wildt et al. (2014) made similar observations for NPF during the photooxidation of a BVOC mix emitted from Mediterranean plants. However, the NO<sub>x</sub> dependence of SOA yield was different from that shown by Wildt et al. (2014). At low-NO<sub>x</sub> concentrations we observed an increasing SOA yield with increasing NO<sub>x</sub> (Fig. 1). At high-NO<sub>x</sub> levels, the yields decreased. Having different NO<sub>x</sub> dependencies at different NO<sub>x</sub> regimes suggests multiple factors at play.

Kroll et al. (2006) suggested that the increase in SOA yield of isoprene with NO<sub>x</sub> could be due to changes in the [NO] / [HO<sub>2</sub>] ratio. As experiments in batch reactors proceed, NO<sub>x</sub> concentrations decrease due to their reactions

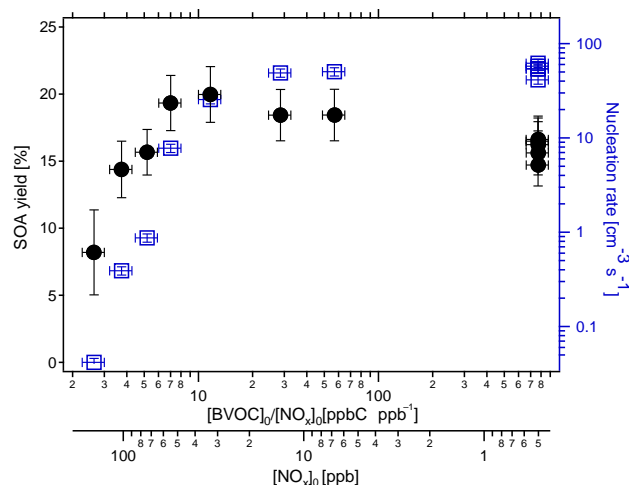


**Figure 1.** Measured SOA yield from PM<sub>max</sub> (black circles) and rates of new particle formation (blue squares) for the β-pinene photooxidation as a function of the ratio of the initial hydrocarbon to the initial NO<sub>x</sub> concentration and as a function of the initial NO<sub>x</sub> concentration. Each point corresponds to one experiment. The errors in nucleation rate and [NO<sub>x</sub>] were estimated to be ±10%. The error in SOA yield was estimated from error propagation using the sum of the systematic error, correction procedure error and error in BVOC data. Note that the horizontal error bars are associated with the BVOC / NO<sub>x</sub> axis.

with OH resulting in a switch from high-NO<sub>x</sub> to low-NO<sub>x</sub> conditions. The lowered NO concentrations cause increasing HO<sub>2</sub> concentrations due to Reaction (R3):



In such experiments, peroxy radicals initially react mainly with NO, whereas peroxy radicals formed later from first generation products, primarily react with HO<sub>2</sub>. Although the reason for the observed increase of SOA yield with increasing NO<sub>x</sub> at low-NO<sub>x</sub> levels was not fully explored, Camredon et al. (2007) noted that this could be due to the influence of OH levels. However, in the majority of studies investigating the impact of NO<sub>x</sub> on SOA formation, OH concentration was either not measured or the potential influence of OH was not discussed in detail (Eddingsaas et al., 2012a, b; Xu et al., 2014).

As the NO<sub>x</sub> concentration is changed in this study, the concentration of OH was found to change markedly (Fig. 2). OH concentrations passed through a maximum (~ 3.8 × 10<sup>7</sup> molecules cm<sup>-3</sup>) at [NO<sub>x</sub>]<sub>ss</sub> ~ 40 ppb ([NO<sub>x</sub>]<sub>0</sub> ~ 70 ppb), which represented a 4-fold increase over that in the absence of NO<sub>x</sub>. NO<sub>x</sub> enhanced OH production in two ways: by increasing [O<sub>3</sub>] and thereby the photolytic OH source, and by recycling OH through Reaction (R3). However, at very high-NO<sub>x</sub> concentrations, NO<sub>x</sub> is acting as a sink for OH due to Reaction (R4):

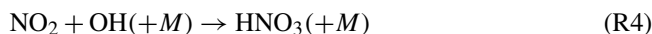


**Table 1.** Experimental conditions and results for  $\beta$ -pinene / NO<sub>x</sub> photooxidation experiments.

$\beta$ -pinene reacted (ppb)	[NO <sub>x</sub> ] <sub>0</sub> (ppb) <sup>a</sup>	[NO <sub>x</sub> ] <sub>ss</sub> (ppb) <sup>b</sup>	[OH] / 10 <sup>7</sup> (cm <sup>-3</sup> )	PM <sub>max</sub> ( $\mu\text{g m}^{-3}$ ) <sup>c</sup>	PM <sub>ss</sub> ( $\mu\text{g m}^{-3}$ ) <sup>d</sup>	J <sub>3</sub> (cm <sup>-3</sup> s <sup>-1</sup> ) <sup>e</sup>	[BVOC] <sub>0</sub> / [NO <sub>x</sub> ] <sub>0</sub> (ppbC ppb <sup>-1</sup> )	SOA yield <sup>f</sup> (%)	SOA yield <sup>g</sup> (%)
33.9	73.9	34.4	3.7	30.3	—	0.9	5.2	15.7	—
34.0	54.8	35.5	3.7	37.6	34.4	7.8	7.0	19.3	17.7
30.4	145.9	86.1	1.8	14.3	—	0.04	2.6	8.2	—
31.4	13.4	9.5	2.2	33.1	31.7	48.9	28.6	18.4	17.7
33.1	102.5	45.7	3.0	27.2	27.2	0.4	3.7	14.4	14.5
33.5	32.9	21.7	3.3	38.2	40.2	25.5	11.7	20.0	21.0
29.4	6.7	5.1	1.5	30.9	30.3	50.3	57.0	18.4	18.0
23.7	< 0.5	< 1.0	0.8	20.0	17.7	41.3	765	14.7	13.1
25.3	< 0.5	< 1.0	0.9	23.5	22.1	57.5	768	16.2	15.3
25.7	< 0.5	< 1.0	0.9	24.4	22.8	62.0	768	16.6	15.5
25.3	< 0.5	< 1.0	0.9	23.8	22.5	54.2	768	16.5	15.6
25.7	< 0.5	< 1.0	1.0	22.9	22.8	53.8	767	15.6	15.5

<sup>a</sup> Initial NO<sub>x</sub> concentration before OH production. <sup>b</sup> NO<sub>x</sub> concentration during steady state, in cases without NO<sub>x</sub> addition we found increasing NO<sub>x</sub>, which is assumed to be produced from residual HNO<sub>3</sub> that is photolyzed by the TUV lamp. <sup>c</sup> Maximum formed particle mass concentration, assuming a SOA density of 1.2 g cm<sup>-3</sup>. These values have been adjusted for wall losses and losses on particles. <sup>d</sup> Particle mass concentration during steady state, assuming an SOA density of 1.2 g cm<sup>-3</sup>. These values have been adjusted for wall losses and losses on particles.

<sup>e</sup> Rates of new particle formation for particles greater than 3 nm. <sup>f</sup> SOA yields determined from PM<sub>max</sub>. <sup>g</sup> SOA yields determined from PM<sub>ss</sub>.

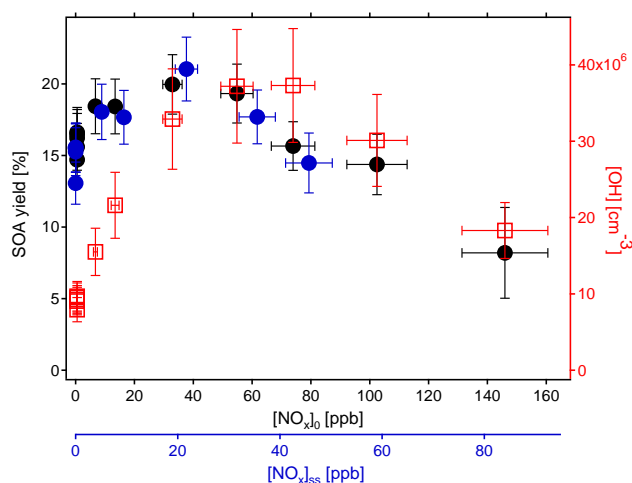


**Figure 2.** Measured SOA yield from PM<sub>max</sub> and from steady state PM (black and blue circles respectively) and measured OH concentration (red squares) as a function of initial ([NO<sub>x</sub>]<sub>0</sub>) and steady state ([NO<sub>x</sub>]<sub>ss</sub>) NO<sub>x</sub> concentrations. The errors in [OH] and [NO<sub>x</sub>] were estimated to be  $\pm 20$  and  $\pm 10$  % respectively. The error in SOA yield was estimated from error propagation using the sum of the systematic error, correction procedure error and error in BVOC data.

Therefore, as illustrated in Fig. 2, OH concentration increased rapidly with increasing NO<sub>x</sub>, reached a maximum value and then decreased gradually. In general terms this is consistent with the nonlinear dependence of OH concentration on NO<sub>x</sub> level in the lower troposphere (Ehhalt and Rohrer, 1995).

It appeared in Fig. 2 that the SOA yields were somehow related to [OH]. Thus, we performed some experiments to further explore the dependence of SOA formation on OH concentration.

### 3.1.1 [OH] dependence of SOA mass formation

To examine whether or not SOA yields depend on the OH concentration, additional experiments were performed at two different OH production rates and the  $\beta$ -pinene concentration varied to give a range of SOA mass. The detailed experimental conditions are summarized in Table 2. Two different  $J(\text{O}^1\text{D})$  conditions ( $1.9 \pm 0.2 \times 10^{-3}$  and  $5.4 \pm 0.5 \times 10^{-3} \text{ s}^{-1}$ ) were used to give significantly different OH production rates at otherwise unchanged conditions. Figure 3 shows particle mass as a function of consumed  $\beta$ -pinene ranging from 20 to 140  $\mu\text{g m}^{-3}$ . Approximately 90–95 % of the total  $\beta$ -pinene was consumed in these experiments.

The OH concentrations were  $4 \times 10^7$ – $1 \times 10^8$  molecules cm<sup>-3</sup> and  $1.1$ – $1.6 \times 10^8$  molecules cm<sup>-3</sup> under low- and high-OH conditions respectively. The SOA yields (incremental yields; see Mentel et al., 2009, and the supplement to this paper) were higher at higher OH levels ( $31 \pm 3$  % and  $20 \pm 1$  % for high- and low-OH conditions respectively).

Increasing yields with increasing OH concentrations have been previously observed. More efficient NPF and/or higher abundance of low volatile vapors at higher oxidant levels were suggested to be the reason. The first should lead to a larger particle surface, which allows for more semi-volatile vapors to condense on particles (Ng et al., 2007b; Healy et al., 2009). As we corrected for wall losses of ELVOCs this effect should be of minor importance in our case. Therefore, other reasons for this dependence have to be considered. Such other reasons might be the secondary reactions (Song et al., 2007; Eddingsaas et al., 2012a, b).

As an example, the rate constant for the reaction of  $\beta$ -pinene + OH ( $k \sim 7.4 \times 10^{-11} \text{ cm}^3 \text{ s}^{-1}$ ; Atkinson and Arey, 2003) is higher than that of the reaction of nopinone + OH ( $k \sim 1.5 \times 10^{-11} \text{ cm}^3 \text{ s}^{-1}$ ; Atkinson and

**Table 2.** Experimental conditions and results for  $\beta$ -pinene photooxidation experiments at two OH levels.

$J(\text{O}^1\text{D}) / 10^{-3} \text{ (s}^{-1}\text{)}^a$	Initial $\beta$ -pinene (ppb)	$\beta$ -pinene reacted (ppb)	$[\text{OH}] / 10^7 \text{ (cm}^{-3}\text{)}$	$\text{PM}_{\text{max}} \text{ (}\mu\text{g m}^{-3}\text{)}^b$
1.9	3.8	3.6	12.5	4.2
1.9	9.2	8.8	11.3	6.5
1.9	9.2	8.9	11.3	6.9
1.9	9.2	8.9	11.3	7.7
1.9	15.9	14.8	6.2	14.4
1.9	24.8	22.0	3.7	23.8
1.9	24.8	22.0	3.7	23.2
1.9	24.8	22.0	3.7	22.0
5.4	3.8	3.6	12.5	4.1
5.4	9.2	9.0	14.5	9.8
5.4	15.9	15.5	15.7	21.3
5.4	24.8	23.9	12.4	39.6

<sup>a</sup>  $J(\text{O}^1\text{D})$  was varied by altering the TUV gap. <sup>b</sup> Maximum formed particle mass concentration, assuming a SOA density of  $1.2 \text{ g cm}^{-3}$ . These values have been adjusted for wall losses and losses on particles.

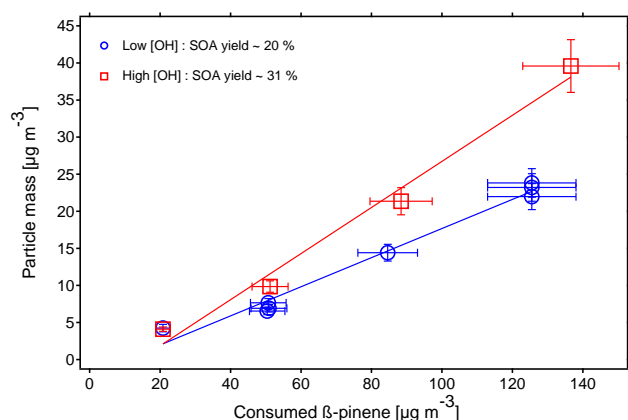


**Figure 3.** Total aerosol mass concentration as a function of the amount of reacted  $\beta$ -pinene under low-[OH] (blue open circles) and high-[OH] (red open squares) conditions. The SOA yield was estimated from the aerosol mass linear regression slope as a function of consumed  $\beta$ -pinene, which resulted in approximately  $20 \pm 1\%$  and  $31 \pm 3\%$  for low- and high-OH conditions respectively. The error in [consumed  $\beta$ -pinene] was estimated to be  $\pm 10\%$  and the error in particle mass was estimated from the sum of the systematic error and the correction procedure error.

Arey, 2003). Nopinone is a major product of  $\beta$ -pinene oxidation. Thus, in the stirred flow reactor, where the oxidation of  $\beta$ -pinene does not go to completion, there is an appreciable concentration of nopinone. Increasing the OH concentration will therefore result in more nopinone consumption and, if nopinone oxidation also forms SOA mass, this additional oxidation forms more SOA mass. As a result, SOA mass will be higher at higher OH concentrations and thus, SOA yield based on the consumption of  $\beta$ -pinene will be higher. Similarly, such sequential OH reactions can also form SOA mass in reactions with other  $\beta$ -pinene oxidation products. Another possibility might be the OH dependence of ELVOC forma-

tion. Formation of such molecules might require more than one OH reaction.

From our data we cannot decide which process plays a major role for the OH dependence of yields. Nevertheless, the results of these experiments affirm the importance of actual OH concentrations in SOA mass formation. This complicates the assignment of the observed changes in SOA yield to the impact of NO<sub>x</sub> on peroxy radical chemistry, as SOA yield was also likely varied with [OH]. Thus, we undertook a series of experiments to decouple the impacts of OH and NO<sub>x</sub> on SOA formation.

### 3.1.2 Isolate the effect of [OH] on SOA formation

To examine the impact of NO<sub>x</sub> on SOA production independent of [OH] changes, a series of experiments were performed where the steady state OH concentration was held constant by tuning the value of  $J(\text{O}^1\text{D})$ . This required constant [OH] monitoring as the system approached steady state, i.e., monitoring the consumption of  $\beta$ -pinene, to ensure the [OH] was adjusted to the desired level. Although there was a significant variation in initial OH concentrations on adding NO<sub>x</sub> if  $J(\text{O}^1\text{D})$  was unchanged, it was possible to maintain the OH concentrations to within 5% across all NO<sub>x</sub> concentrations by adjusting  $J(\text{O}^1\text{D})$  (Fig. 4). Figure 5 shows the SOA yield as a function of [NO<sub>x</sub>] during the steady state before and after [OH] adjustment. Before adjusting [OH] the yield profile was consistent with our previous results; SOA yield increased with increasing NO<sub>x</sub> at low-NO<sub>x</sub> levels and then dropped at high-NO<sub>x</sub> levels. After adjusting [OH], the yield revealed no increase at low-NO<sub>x</sub> levels. It was only suppressed by increasing NO<sub>x</sub>. This indicated that the observed increase in SOA yield without adjusting [OH] is a result of NO<sub>x</sub> enhancing [OH]. Thus, isolating the effect of [OH] revealed that increasing [NO<sub>x</sub>] only suppressed particle mass formation, and therefore also suppressed SOA mass yield.

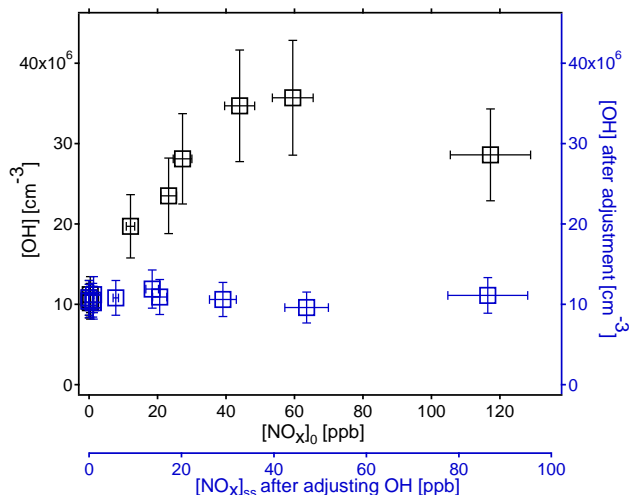
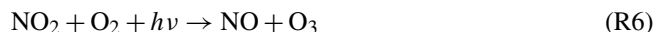


**Figure 4.** Comparison of [OH] before (black squares) and after (blue squares) adjusting OH concentration during steady state in NO<sub>x</sub> experiments. The errors in [OH] and [NO<sub>x</sub>] were estimated to be ±20 and ±10 % respectively.

### 3.2 Possible role of peroxy radical chemistry and [NO] / [NO<sub>2</sub>] ratio in SOA formation

We also investigated the effect of the [NO] / [NO<sub>2</sub>] ratio on SOA formation from β-pinene / NO<sub>x</sub> mixtures. To change this ratio we changed [O<sub>3</sub>]. Ozone, NO and NO<sub>2</sub> are interrelated as illustrated in Reactions (R5) and (R6):



Hence, to a good approximation the [NO] / [NO<sub>2</sub>] ratio is described by the photostationary steady state (Leighton, 1961):

$$\frac{[\text{NO}]}{[\text{NO}_2]} = \frac{J(\text{NO}_2)}{k^5 [\text{O}_3]}, \quad (4)$$

where  $J(\text{NO}_2)$  represents the photolysis rate of NO<sub>2</sub> and  $k^5$  is the rate coefficient of Reaction (R5). Hence, adjusting [O<sub>3</sub>] in the chamber allowed varying [NO] / [NO<sub>2</sub>] ratios. Here, to probe the dependency of SOA mass formation on relative NO and NO<sub>2</sub> concentrations, NO<sub>x</sub> experiments were performed with approximately 50 % higher O<sub>3</sub> concentration ( $74 \pm 7$  ppb, [NO] / [NO<sub>2</sub>] =  $0.018 \pm 0.004$  ppb ppb<sup>-1</sup>) than that of previous NO<sub>x</sub> experiments where the [NO] / [NO<sub>2</sub>] ratio was  $0.035 \pm 0.005$  ppb ppb<sup>-1</sup>. The remaining conditions maintained the same.

Results obtained from these experiments are shown in Fig. 6. The behavior observed in the high-O<sub>3</sub> experiments (equivalent to lower NO / NO<sub>2</sub>) was different from that in the experiments with lower [O<sub>3</sub>] (cf. Figs. 6 to 4). When not adjusted, [OH] increased with increasing NO<sub>x</sub> but the increase was less pronounced. With a lower [NO] / [NO<sub>2</sub>]

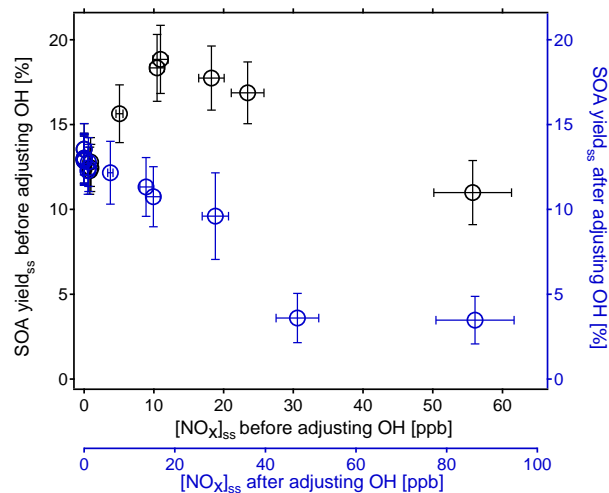


**Figure 5.** Comparison of SOA yield before (black circles) and after (blue circles) adjusting OH concentration during steady state in NO<sub>x</sub> experiments. The error in [NO<sub>x</sub>] was estimated to be ±10 % and the error in SOA yield was estimated from error propagation using the sum of the systematic error, correction procedure error and error in BVOC data.

ratio, the maximum OH concentration increase was approximately 2-fold relative to the respective NO<sub>x</sub>-free experiments (Fig. 6), compared to the 4-fold increase with the higher [NO] / [NO<sub>2</sub>] (Fig. 4). This is consistent with the assumption that Reaction (R3) recycles OH. There was also a slight increase in SOA yield when [NO<sub>x</sub>] increased up to ~15 ppb (Fig. 7). In addition, the increase in SOA yield was less pronounced in the high-O<sub>3</sub> experiments again pointing to the role of [OH] in SOA formation.

After adjusting [OH] to the same level as in the NO<sub>x</sub>-free experiments (Fig. 6), no increase in SOA yield was observed and increasing NO<sub>x</sub> only suppressed SOA formation (Fig. 7). These results were consistent with those found earlier in the low-O<sub>3</sub> experiments indicating that, after isolating the effect of [OH], SOA yield was only suppressed with increasing NO<sub>x</sub> also at higher [O<sub>3</sub>]. Comparing the yield profiles obtained from the low-O<sub>3</sub> and the high-O<sub>3</sub> experiments respectively (blue circles in Figs. 5 and 7), it can be seen that the decrease in SOA yield was ~35 % in the high-O<sub>3</sub> experiments, whereas it was roughly 70 % in the low-O<sub>3</sub> experiments. This shows that NO<sub>x</sub> dependencies itself depend on the composition of NO<sub>x</sub>. As the suppression of yield was more pronounced in the low-O<sub>3</sub> experiments (i.e., higher [NO] / [NO<sub>2</sub>]), it indicates that NO is the molecule mainly responsible for the SOA yield diminishing effect of NO<sub>x</sub>.

After separating the impacts of NO<sub>x</sub> on OH, there was a remaining effect on SOA formation. According to present knowledge (e.g., Hatakeyama et al., 1991; Pandis et al., 1991; Kroll et al., 2006) this effect is due to impacts of NO<sub>x</sub> on RO<sub>2</sub> chemistry. The most obvious impact of NO<sub>x</sub> is the change in product composition. Organic nitrates are formed as an al-

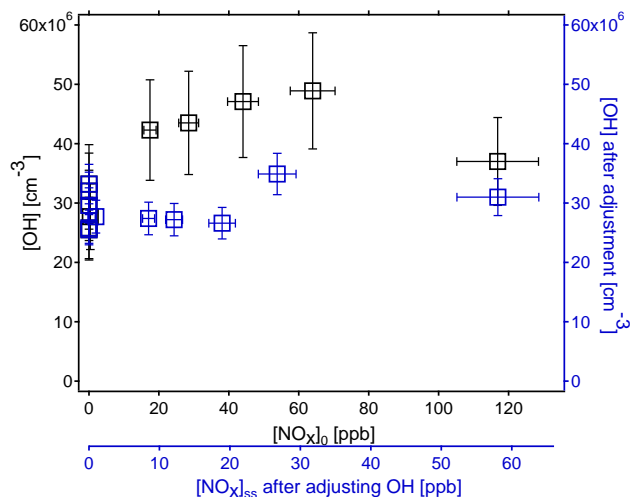


**Figure 6.** Comparison of [OH] before (black squares) and after (blue squares) adjusting OH concentration during steady state in  $\text{NO}_x$  experiments performed under lower  $[\text{NO}] / [\text{NO}_2]$  ratio. The errors in [OH] and  $[\text{NO}_x]$  were estimated to be  $\pm 20$  and  $\pm 10\%$  respectively.

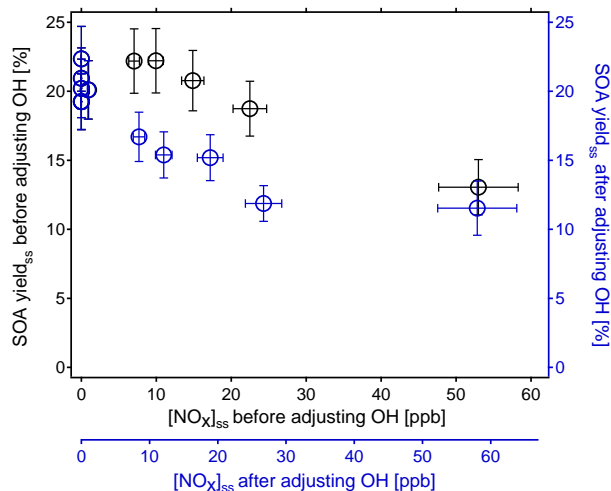


**Figure 7.** Comparison of SOA yield before (black circles) and after (blue circles) adjusting OH concentration during steady state in  $\text{NO}_x$  experiments performed under lower  $[\text{NO}] / [\text{NO}_2]$  ratio. The error in  $[\text{NO}_x]$  was estimated to be  $\pm 10\%$  and the error in SOA yield was estimated from error propagation using the sum of the systematic error, correction procedure error and error in BVOC data.

ternative to hydroperoxides and formation of organic nitrates may have an effect on the average volatility of the product mixture. Also decomposition of alkoxy radicals may play a role here. Decomposition of alkoxy radicals can lead to products with higher volatility and thus to a mixture with an average higher volatility.

We found that diminishing of SOA is more effective at higher  $[\text{NO}] / [\text{NO}_2]$ . This points to NO as a major player and

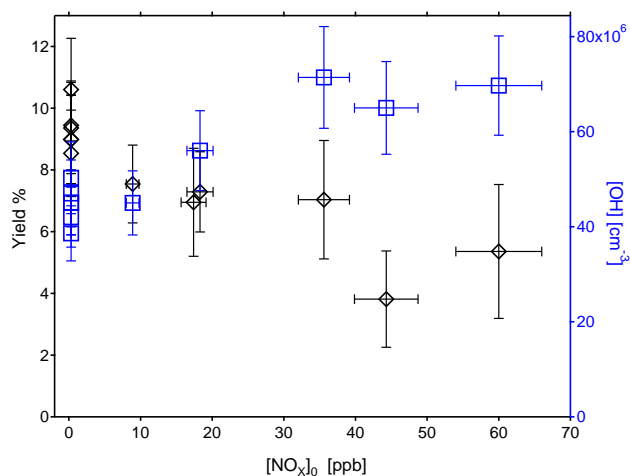


**Figure 8.** Measured SOA yield (black diamonds) and measured OH concentration (blue squares) as a function of initial  $\text{NO}_x$  concentration for  $\alpha$ -pinene /  $\text{NO}_x$  photooxidation experiments. Note that, due to the lower  $\alpha$ -pinene concentrations, the  $x$  axis is not equivalent to the  $x$  axes of Figs. 5 and 7. In the sense of BVOC /  $\text{NO}_x$  ratios, the  $\text{NO}_x$  range scanned here is  $\sim 3$  times higher. The errors in [OH] and  $[\text{NO}_x]$  were estimated to be  $\pm 15$  and  $\pm 10\%$  respectively. The error in SOA yield was estimated from error propagation using the sum of the systematic error, correction procedure error and error in BVOC data.

thus to a role of alkoxy radical decomposition. As alkoxy radicals are produced by only  $\text{RO}_2 + \text{NO}$  reactions, more effective suppression of SOA formation at higher  $[\text{NO}] / [\text{NO}_2]$  would be consistent with alkoxy radical decomposition leading to decomposition products with on average high vapor pressures. However, from our results no clear conclusion can be given in this respect.

### 3.3 Comparison of the impact of $\text{NO}_x$ on SOA yield from $\alpha$ -pinene and $\beta$ -pinene photooxidation

A series of  $\alpha$ -pinene /  $\text{NO}_x$  experiments were performed in the same chamber to compare the  $\text{NO}_x$  dependencies of SOA formation of  $\alpha$ -pinene to that of  $\beta$ -pinene. These experiments were performed with  $12 \pm 1.2$  ppb  $\alpha$ -pinene,  $78 \pm 14$  ppb  $\text{O}_3$  and with  $[\text{NO}_x]_0$  up to 126 ppb.

When using  $\alpha$ -pinene as the SOA precursor, no increase in aerosol mass formation was observed at low  $\text{NO}_x$ , with only suppression of the particle mass formation and the SOA yield (Fig. 8). Furthermore, presumably due to the lower  $\alpha$ -pinene concentrations, no particle formation at all was observed when  $[\text{NO}_x]_0$  was above 60 ppb.

At high- $\text{NO}_x$  levels, the differences between the  $\text{NO}_x$  dependencies of  $\alpha$ -pinene (Fig. 8) and  $\beta$ -pinene (Fig. 1) photooxidation were not very strong, both showing a decrease with increasing  $\text{NO}_x$ . At low- $\text{NO}_x$  levels there were substantial differences, in that  $\beta$ -pinene showed a distinctive increase and maximum of the yield, while the yield of  $\alpha$ -



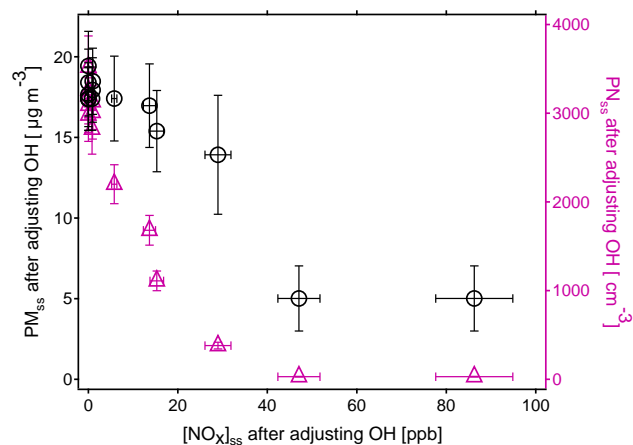


**Figure 9.** Comparison of measured particle mass and particle number concentration after adjusting [OH] as a function of [NO<sub>x</sub>] during steady state in the absence of seed aerosol. The error in particle number concentration was estimated to be ±10 %.

pinene is almost unaffected and monotonically decreasing. A part of these differences can be explained by the differences in [O<sub>3</sub>] during α-pinene and β-pinene photooxidation. The lower [O<sub>3</sub>] in the β-pinene experiments caused higher [NO]/[NO<sub>2</sub>] ratios and thus more effective conversion of HO<sub>2</sub> to OH by NO (Reaction R3). This is supported by the experiments with β-pinene performed at higher [O<sub>3</sub>] that caused a less NO<sub>x</sub>-induced increase of [OH] (Fig. 6, black squares), as well as less NO<sub>x</sub>-induced increase of SOA yield (Fig. 7, black circles). Restricting focus to the same [BVOC]/[NO<sub>x</sub>] where the substantial increase in β-pinene SOA yield was observed (> 100 to ~ 20 ppbC ppb<sup>-1</sup>), such increases were neither observed for α-pinene nor for the monoterpene mix emitted from Mediterranean species (Wildt et al., 2014). The NO<sub>x</sub> dependence of SOA formation therefore is different in different chemical systems. Different impacts of NO<sub>x</sub> superimpose each other and the net effect of NO<sub>x</sub> is determined by the strongest impact in the individual chemical system. For SOA formation from α-pinene, the suppressing effect via impacts on peroxy radical chemistry was obviously stronger than the increases in SOA yield by NO<sub>x</sub>-induced increases of [OH]. However, at high-NO<sub>x</sub> conditions, the principle behavior of all systems was identical; a general SOA yield suppression with increasing NO<sub>x</sub>.

### 3.4 Impact of NO<sub>x</sub> on SOA formation in the presence of seed aerosol

From Fig. 2, it can be seen that the SOA yield measured at [NO<sub>x</sub>]<sub>ss</sub> ~ 86 ppb ([NO<sub>x</sub>]<sub>0</sub> ~ 146 ppb) was lower than that at [NO<sub>x</sub>]<sub>0</sub> < 1 ppb while [OH] was higher. Hence, there must be another effect of NO<sub>x</sub> addition besides its impact on [OH]. As illustrated in Fig. 9, particle number concentrations were suppressed significantly when adding NO<sub>x</sub>. The strong de-

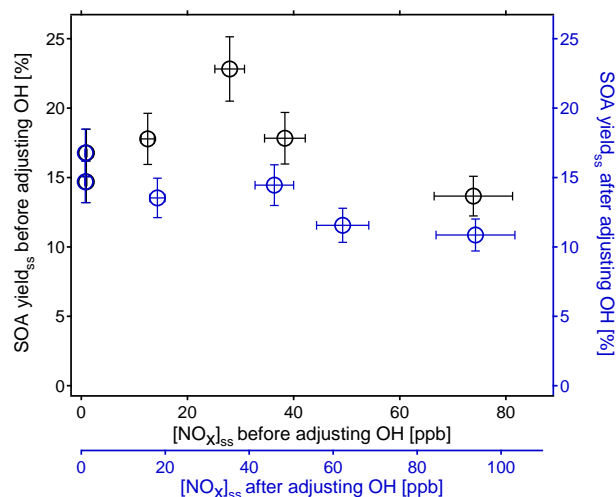


**Figure 10.** Comparison of SOA yield before (black circles) and after (blue circles) adjusting OH concentration during steady state in NO<sub>x</sub> experiments performed in the presence of seed aerosol. The error in [NO<sub>x</sub>] was estimated to be ±10 % and the error in SOA yield was estimated from error propagation using the sum of the systematic error, correction procedure error and error in BVOC data.

crease of particle number concentration with increasing NO<sub>x</sub> indicates that NPF is suppressed by NO<sub>x</sub> (see also Wildt et al., 2014). Hence, there is a high chance that the SOA formation is hindered by low particle phase condensational sinks at high-NO<sub>x</sub> levels, and thus the observed suppression of SOA yield may be due to the lowering of available particle surface. At high-NO<sub>x</sub> conditions, particle numbers and surfaces were quite low. Therefore, high correction factors had to be used to correct the particle mass for wall losses of ELVOCs, which includes high uncertainties (see Supplement). These uncertainties can be diminished by using seed particles since they provide a surface onto which the low volatile organics may condense. In the presence of seed aerosol, the growth of particles would not be limited by the surface of particles and would be much less affected by losses of SOA precursors on the chamber walls.

Therefore, experiments with variations of [NO<sub>x</sub>] were also conducted in the presence of ammonium sulfate ((NH<sub>4</sub>)<sub>2</sub>SO<sub>4</sub>) seed particles (average seed mass and surface were approximately 9 ± 1 μg m<sup>-3</sup> and 1.3 × 10<sup>-3</sup> m<sup>2</sup> m<sup>-3</sup> respectively). These experiments were carried out in the same manner as previous experiments: by adjusting [OH] during steady state to the same level as during the NO<sub>x</sub>-free experiments. Figure 10 presents a comparison of SOA yield before and after [OH] adjustment for seeded NO<sub>x</sub> experiments (seed mass is subtracted from the total particle mass to determine the organic mass used in the yield calculation). The results from the seeded experiments showed the same general features as the unseeded experiments. Without adjustment of [OH], yields increased with increasing NO<sub>x</sub> at low levels and were slightly suppressed with further increas-

ing NO<sub>x</sub>. The most evident difference here to the experiments without seed particles is the fairly high yield at high [NO<sub>x</sub>] (Fig. 10). Even after [OH] was adjusted, the decrease in SOA yield was not as significant as in the experiments without seed particles. This suggests that in the absence of seed particles, the accumulation of mass was indeed limited by low particle surface caused by the NO<sub>x</sub>-induced suppression of NPF.

In the presence of seed particles and at constant [OH], the decrease in yield was only moderate. This indicates that other NO<sub>x</sub> impacts such as formation of organic nitrates were moderate as well. The difference between yields determined with and without addition of seed particles indicates that at very small particle surface, our correction procedure underestimates wall losses of precursors. This might be due to either possible differences in uptake of the ELVOC by particles (mainly organic particles vs. ammonium sulfate particles), or the differences in the size of particles. However, the real reason for this underestimation is not known yet.

Our correction procedure may involve uncertainties and errors. Nevertheless, it had to be applied; otherwise the NO<sub>x</sub> dependence would have been overestimated. NO<sub>x</sub> suppresses NPF and thereby limits mass formation in the absence of seed particles. As both, the impacts of wall losses and impacts of suppressed NPF on SOA mass formation are certainly diminished in the presence of seed, we assume that the experiments with seed particles give the most reliable results on NO<sub>x</sub> impacts on SOA mass formation from  $\beta$ -pinene.

#### 4 Summary and conclusions

We investigated the effect of NO<sub>x</sub> on SOA formation from  $\beta$ -pinene photooxidation under low-NO<sub>x</sub> and high-NO<sub>x</sub> conditions and found a very similar behavior as that observed in other studies (Pandis et al., 1991; Zhang et al., 1992; Presto et al., 2005; Kroll et al., 2006; Camredon et al., 2007; Pathak et al., 2007; Chan et al., 2010; Hoyle et al., 2011; Loza et al., 2014). At low-NO<sub>x</sub> levels SOA yields increased with increasing NO<sub>x</sub> and then decreased at higher NO<sub>x</sub> concentrations. The increase of yield at low [NO<sub>x</sub>] was caused by the NO<sub>x</sub>-induced increase of [OH]. The decrease of yield at higher NO<sub>x</sub> levels was mainly a consequence of NPF suppression and thereby decreasing particle condensational sink with increasing NO<sub>x</sub>. Eliminating the impacts of NO<sub>x</sub> on NPF and on [OH], showed that the impacts of NO<sub>x</sub> on mass formation were only moderate. Even at the highest NO<sub>x</sub> level ([NO<sub>x</sub>]<sub>ss</sub> ~ 86 ppb, [BVOC]<sub>ss</sub> / [NO<sub>x</sub>]<sub>ss</sub> ~ 1.1) suppression of mass yield was only 20–30%. VOC / NO<sub>x</sub> ratios in typical urban air are often much higher than the lower end of the [BVOC] / [NO<sub>x</sub>] range used here (Cai et al., 2011; Pollack et al., 2013; Zou et al., 2015). Therefore, depending on the conditions, impacts of NO<sub>x</sub> on SOA formation in the real atmosphere may be far less than 20–30%.

Our study also showed that SOA yield is dependent on OH concentration. Although the exact mechanism for this [OH] dependence is still unknown, our results show that besides yield dependencies on the amount of pre-existing matter and effects like partitioning there is also a dependence on reaction conditions, in particular on oxidant levels. Although SOA yields measured in laboratory chambers may not be indicative of the yields in the real atmosphere, their variations as a consequence of different conditions could provide a more comprehensive description of SOA in global and climate model.

#### 5 Data availability

All data given in figures can be displayed in tables or in digital form. This includes the data given in the Supplement where we describe the method how the mass yields were corrected for wall losses of ELVOCs. Please send all requests for data to J.wildt@fz-juelich.de.

**The Supplement related to this article is available online at doi:10.5194/acp-16-11237-2016-supplement.**

*Acknowledgements.* This work was supported by the European Commission's 7th Framework Program under grant agreement no. 287382 (Marie Curie Training Network PIMMS).

The article processing charges for this open-access publication were covered by a Research Centre of the Helmholtz Association.

Edited by: N. L. Ng

Reviewed by: two anonymous referees

#### References

- Atkinson, R. and Arey, J.: Atmospheric degradation of volatile organic compounds, *Chem. Rev.*, 103, 4605–4638, doi:10.1021/cr0206420, 2003.
- Cai, C., Kelly, J. T., Avise, J. C., Kaduwela, A. P., and Stockwell, W. R.: Photochemical modeling in California with two chemical mechanisms: model intercomparison and response to emission reductions, *J. Air Waste Manage.*, 61, 559–572, doi:10.3155/1047-3289.61.5.559, 2011.
- Camredon, M., Aumont, B., Lee-Taylor, J., and Madronich, S.: The SOA/VOC/NO<sub>x</sub> system: an explicit model of secondary organic aerosol formation, *Atmos. Chem. Phys.*, 7, 5599–5610, doi:10.5194/acp-7-5599-2007, 2007.
- Chan, A. W. H., Chan, M. N., Surratt, J. D., Chhabra, P. S., Loza, C. L., Crouse, J. D., Yee, L. D., Flagan, R. C., Wennberg, P. O., and Seinfeld, J. H.: Role of aldehyde chemistry and NO<sub>x</sub> concentrations in secondary organic aerosol formation, *Atmos. Chem. Phys.*, 10, 7169–7188, doi:10.5194/acp-10-7169-2010, 2010.

- Davidson, J. A., Cantrell, C. A., McDaniel, A. H., Shetter, R. E., Madronich, S., and Calvert, J. G.: Visible-ultraviolet absorption cross sections for NO<sub>2</sub> as a function of temperature, *J. Geophys. Res.-Atmos.*, 93, 7105–7112, doi:10.1029/JD093iD06p07105, 1988.
- Eddingsaas, N. C., Loza, C. L., Yee, L. D., Chan, M., Schilling, K. A., Chhabra, P. S., Seinfeld, J. H., and Wennberg, P. O.:  $\alpha$ -pinene photooxidation under controlled chemical conditions – Part 2: SOA yield and composition in low- and high-NO<sub>x</sub> environments, *Atmos. Chem. Phys.*, 12, 7413–7427, doi:10.5194/acp-12-7413-2012, 2012a.
- Eddingsaas, N. C., Loza, C. L., Yee, L. D., Seinfeld, J. H., and Wennberg, P. O.:  $\alpha$ -pinene photooxidation under controlled chemical conditions – Part 1: Gas-phase composition in low- and high-NO<sub>x</sub> environments, *Atmos. Chem. Phys.*, 12, 6489–6504, doi:10.5194/acp-12-6489-2012, 2012b.
- Ehhalt, D. H. and Rohrer, F.: The impact of commercial aircraft on tropospheric ozone, in: *The Chemistry of the Atmosphere – Oxidants and Oxidation in the Earth's Atmosphere*, edited by: Bandy, A. R., The Royal Society of Chemistry, Special Publication No. 170, 105–120, 1995.
- Ehn, M., Thornton, J. A., Kleist, E., Sipilä, M., Junninen, H., Pullinen, I., Springer, M., Rubach, F., Tillmann, R., Lee, B., Lopez-Hilfiker, F., Andres, S., Acir, I.-H., Rissanen, M., Jokinen, T., Schobesberger, S., Kangasluoma, J., Kontkanen, J., Nieminen, T., Kurtén, T., Nielsen, L. B., Jørgensen, S., Kjaergaard, H. G., Canagaratna, M., Maso, M. D., Berndt, T., Petäjä, T., Wahner, A., Kerminen, V.-M., Kulmala, M., Worsnop, D. R., Wildt, J., and Mentel, T. F.: A large source of low-volatility secondary organic aerosol, *Nature*, 506, 476–479, doi:10.1038/nature13032, 2014.
- Griffin, R. J., Cocker, D. R., Seinfeld, J. H., and Dabdub, D.: Estimate of global atmospheric organic aerosol from oxidation of biogenic hydrocarbons, *Geophys. Res. Lett.*, 26, 2721–2724, doi:10.1029/1999GL900476, 1999a.
- Griffin, R. J., Cocker, D. R., Flagan, R. C., and Seinfeld, J. H.: Organic aerosol formation from the oxidation of biogenic hydrocarbons, *J. Geophys. Res.*, 104, 3555–3567, doi:10.1029/1998JD100049, 1999b.
- Guenther, A., Hewitt, C. N., Erickson, D., Fall, R., Geron, C., Graedel, T., Harley, P., Klinger, L., Lerdau, M., McKay, W. A., Pierce, T., Scholes, B., Steinbrecher, R., Tallamraju, R., Taylor, J., and Zimmerman, P.: A global model of natural volatile organic compound emissions, *J. Geophys. Res.*, 100, 8873–8892, doi:10.1029/94JD02950, 1995.
- Guenther, A. B., Jiang, X., Heald, C. L., Sakulyanontvittaya, T., Duhl, T., Emmons, L. K., and Wang, X.: The Model of Emissions of Gases and Aerosols from Nature version 2.1 (MEGAN2.1): an extended and updated framework for modeling biogenic emissions, *Geosci. Model Dev.*, 5, 1471–1492, doi:10.5194/gmd-5-1471-2012, 2012.
- Hallquist, M., Wenger, J. C., Baltensperger, U., Rudich, Y., Simpson, D., Claeys, M., Dommen, J., Donahue, N. M., George, C., Goldstein, A. H., Hamilton, J. F., Herrmann, H., Hoffmann, T., Iinuma, Y., Jang, M., Jenkin, M. E., Jimenez, J. L., Kiendler-Scharr, A., Maenhaut, W., McFiggans, G., Mentel, Th. F., Monod, A., Prévôt, A. S. H., Seinfeld, J. H., Surratt, J. D., Szmigielski, R., and Wildt, J.: The formation, properties and impact of secondary organic aerosol: current and emerging issues, *Atmos. Chem. Phys.*, 9, 5155–5236, doi:10.5194/acp-9-5155-2009, 2009.
- Hatakeyama, S., Izumi, K., Fukuyama, T., Akimoto, H., and Washida, N.: Reactions of OH with  $\alpha$ -pinene and  $\beta$ -pinene in air: Estimate of global CO production from the atmospheric oxidation of terpenes, *J. Geophys. Res.*, 96, 947–958, doi:10.1029/90JD02341, 1991.
- Healy, R. M., Temime, B., Kuprovskite, K., and Wenger, J. C.: Effect of Relative Humidity on Gas/Particle Partitioning and Aerosol Mass Yield in the Photooxidation of p-Xylene. *Environ. Sci. Technol.*, 43, 1884–1889, 2009.
- Hoffmann, T., Klockow, D., Odum, J., Bowman, F., Collins, D., Flagan, R. C., and Seinfeld, J. H.: Formation of Organic Aerosols from the Oxidation of Biogenic Hydrocarbons, *J. Atmos. Chem.*, 26, 189–222, doi:10.1023/A:1005734301837, 1997.
- Hoyle, C. R., Boy, M., Donahue, N. M., Fry, J. L., Glasius, M., Guenther, A., Hallar, A. G., Huff Hartz, K., Petters, M. D., Petäjä, T., Rosenoern, T., and Sullivan, A. P.: A review of the anthropogenic influence on biogenic secondary organic aerosol, *Atmos. Chem. Phys.*, 11, 321–343, doi:10.5194/acp-11-321-2011, 2011.
- Johnson, D., Jenkin, M. E., Wirtz, K., and Martin-Reviejo, M.: Simulating the Formation of Secondary Organic Aerosol from the Photooxidation of Aromatic Hydrocarbons, *Environ. Chem.*, 2, 35–48, 2005.
- Kiendler-Scharr, A., Wildt, J., Dal Maso, M., Hohaus, T., Kleist, E., Mentel, T. F., Tillmann, R., Uerlings, R., Schurr, U., and Wahner, A.: New particle formation in forests inhibited by isoprene emissions, *Nature*, 461, 381–384, doi:10.1038/nature08292, 2009.
- Kroll, J. H., Ng, N. L., Murphy, S. M., Flagan, R. C., and Seinfeld, J. H.: Secondary organic aerosol formation from Isoprene photooxidation, *Environ. Sci. Technol.*, 40, 1869–1877, doi:10.1021/es0524301, 2006.
- Larsen, B. R., Di Bella, D., Glasius, M., Winterhalter, R., Jensen, N. R., and Hjorth, J.: Gas-phase OH oxidation of monoterpenes: Gaseous and particulate products, *J. Atmos. Chem.*, 38, 231–276, doi:10.1023/A:1006487530903, 2001.
- Leighton, P. A.: *photochemistry of Air pollution*, Academic press, New York and London, 1961.
- Loza, C. L., Craven, J. S., Yee, L. D., Coggon, M. M., Schwantes, R. H., Shiraiwa, M., Zhang, X., Schilling, K. A., Ng, N. L., Canagaratna, M. R., Ziemann, P. J., Flagan, R. C., and Seinfeld, J. H.: Secondary organic aerosol yields of 12-carbon alkanes, *Atmos. Chem. Phys.*, 14, 1423–1439, doi:10.5194/acp-14-1423-2014, 2014.
- Master Chemical Mechanism (MCM): version 3.3.1, available at: <http://mcm.leeds.ac.uk/MCM/roots.htm>, last access: June 2016.
- Mentel, Th. F., Wildt, J., Kiendler-Scharr, A., Kleist, E., Tillmann, R., Dal Maso, M., Fisseha, R., Hohaus, Th., Spahn, H., Uerlings, R., Wegener, R., Griffiths, P. T., Dinar, E., Rudich, Y., and Wahner, A.: Photochemical production of aerosols from real plant emissions, *Atmos. Chem. Phys.*, 9, 4387–4406, doi:10.5194/acp-9-4387-2009, 2009.
- Mentel, T. F., Springer, M., Ehn, M., Kleist, E., Pullinen, I., Kurtén, T., Rissanen, M., Wahner, A., and Wildt, J.: Formation of highly oxidized multifunctional compounds: autoxidation of peroxy radicals formed in the ozonolysis of alkenes – deduced from structure-product relationships, *Atmos. Chem. Phys.*, 15, 6745–6765, doi:10.5194/acp-15-6745-2015, 2015.

- Ng, N. L., Chhabra, P. S., Chan, A. W. H., Surratt, J. D., Kroll, J. H., Kwan, A. J., McCabe, D. C., Wennberg, P. O., Sorooshian, A., Murphy, S. M., Dalleska, N. F., Flagan, R. C., and Seinfeld, J. H.: Effect of NO<sub>x</sub> level on secondary organic aerosol (SOA) formation from the photooxidation of terpenes, *Atmos. Chem. Phys.*, 7, 5159–5174, doi:10.5194/acp-7-5159-2007, 2007a.
- Ng, N. L., Kroll, J. H., Chan, A. W. H., Chhabra, P. S., Flagan, R. C., and Seinfeld, J. H.: Secondary organic aerosol formation from m-xylene, toluene, and benzene, *Atmos. Chem. Phys.*, 7, 3909–3922, doi:10.5194/acp-7-3909-2007, 2007b.
- Odum, J. R., Hoffmann, T., Bowman, F., Collins, D., Flagan, R. C., and Seinfeld, J. H.: Gas/Particle partitioning and secondary organic aerosol yields, *Environ. Sci. Technol.*, 30, 2580–2585, doi:10.1021/es950943+, 1996.
- Pandis, S. N., Paulson, S. E., Seinfeld, J. H., and Flagan, R. C.: Aerosol formation in the photooxidation of isoprene and  $\beta$ -pinene, *Atmos. Environ. A-Gen.*, 25, 997–1008, doi:10.1016/0960-1686(91)90141-S, 1991.
- Pathak, R. K., Presto, A. A., Lane, T. E., Stanier, C. O., Donahue, N. M., and Pandis, S. N.: Ozonolysis of  $\alpha$ -pinene: parameterization of secondary organic aerosol mass fraction, *Atmos. Chem. Phys.*, 7, 3811–3821, doi:10.5194/acp-7-3811-2007, 2007.
- Pollack, I. B., Ryerson, T. B., Trainer, M., Neuman, J. A., Roberts, J. M., and Parrish, D. D.: Trends in ozone, its precursors, and related secondary oxidation products in Los Angeles, California: A synthesis of measurements from 1960 to 2010, *J. Geophys. Res.-Atmos.*, 118, 5893–5911, doi:10.1002/jgrd.50472, 2013.
- Presto, A. A., Huff Hartz, K. E., and Donahue, N. M.: Secondary organic aerosol production from terpene ozonolysis. 2. Effect of NO<sub>x</sub> concentration, *Environ. Sci. Technol.*, 39, 7046–7054, doi:10.1021/es050400s, 2005.
- Song, C., Na, K., Warren, B., Malloy, Q., and Cocker, D. R.: Impact of propene on secondary organic aerosol formation from m-xylene, *Environ. Sci. Technol.*, 41, 6990–6995, doi:10.1021/Es062279a, 2007.
- Wildt, J., Mentel, T. F., Kiendler-Scharr, A., Hoffmann, T., Andres, S., Ehn, M., Kleist, E., M $\ddot{u}$ sgen, P., Rohrer, F., Rudich, Y., Springer, M., Tillmann, R., and Wahner, A.: Suppression of new particle formation from monoterpene oxidation by NO<sub>x</sub>, *Atmos. Chem. Phys.*, 14, 2789–2804, doi:10.5194/acp-14-2789-2014, 2014.
- Xu, L., Kollman, M. S., Song, C., Shilling, J. E., and Ng, N. L.: Effects of NO<sub>x</sub> on the Volatility of Secondary Organic Aerosol from Isoprene Photooxidation, *Environ. Sci. Technol.*, 48, 2253–2262, doi:10.1021/es404842g, 2014.
- Zhang, S.-H., Shaw, M., Seinfeld, J. H., and Flagan, R. C.: Photochemical aerosol formation from  $\alpha$ -pinene- and  $\beta$ -pinene, *J. Geophys. Res.*, 97, 20717–20729, doi:10.1029/92JD02156, 1992.
- Zou, Y., Deng, X. J., Zhu, D., Gong, D. C., Wang, H., Li, F., Tan, H. B., Deng, T., Mai, B. R., Liu, X. T., and Wang, B. G.: Characteristics of 1 year of observational data of VOCs, NO<sub>x</sub> and O<sub>3</sub> at a suburban site in Guangzhou, China, *Atmos. Chem. Phys.*, 15, 6625–6636, doi:10.5194/acp-15-6625-2015, 2015.